

Advanced Materials and Devices for Bioresorbable Electronics

Published as part of the *Accounts of Chemical Research* special issue “*The Interface of Biology with Nanoscience and Electronics*”.

Seung-Kyun Kang,^{†,⊥} Jahyun Koo,^{‡,⊥} Yoon Kyeong Lee,[§] and John A. Rogers^{*,‡,§,||} 

[†]Department of Bio and Brain Engineering, Korea Advanced Institute of Science and Technology, Daejeon 34141, Republic of Korea

[‡]Center for Bio-Integrated Electronics, Northwestern University, Evanston, Illinois 60208, United States

[§]Department of Chemistry, University of Illinois at Urbana–Champaign, Urbana, Illinois 61801, United States

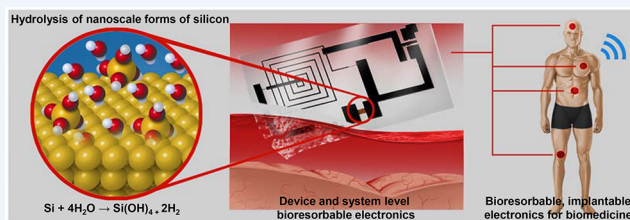
^{||}Departments of Materials Science & Engineering and Mechanical Engineering, Northwestern University, Evanston, Illinois 60208, United States

CONSPECTUS: Recent advances in materials chemistry establish the foundations for unusual classes of electronic systems, characterized by their ability to fully or partially dissolve, disintegrate, or otherwise physically or chemically decompose in a controlled fashion after some defined period of stable operation. Such types of “transient” technologies may enable consumer gadgets that minimize waste streams associated with disposal, implantable sensors that disappear harmlessly in the body, and hardware-secure platforms that prevent unwanted recovery of sensitive data. This second area of opportunity, sometimes referred to as bioresorbable electronics, is of particular interest due to its ability to provide diagnostic or therapeutic function in a manner that can enhance or monitor transient biological processes, such as wound healing, while bypassing risks associated with extended device load on the body or with secondary surgical procedures for removal.

Early chemistry research established sets of bioresorbable materials for substrates, encapsulation layers, and dielectrics, along with several options in organic and bio-organic semiconductors. The subsequent realization that nanoscale forms of device-grade monocrystalline silicon, such as silicon nanomembranes (m-Si NMs, or Si NMs) undergo hydrolysis in biofluids to yield biocompatible byproducts over biologically relevant time scales advanced the field by providing immediate routes to high performance operation and versatile, sophisticated levels of function. When combined with bioresorbable conductors, dielectrics, substrates, and encapsulation layers, Si NMs provide the basis for a broad, general class of bioresorbable electronics. Other properties of Si, such as its piezoresistivity and photovoltaic properties, allow other types of bioresorbable devices such as solar cells, strain gauges, pH sensors, and photodetectors. The most advanced bioresorbable devices now exist as complete systems with successful demonstrations of clinically relevant modes of operation in animal models.

This Account highlights the foundational materials concepts for this area of technology, starting with the dissolution chemistry and reaction kinetics associated with hydrolysis of Si NMs as a function of temperature, pH, and ion and protein concentration. A following discussion focuses on key supporting materials, including a range of dielectrics, metals, and substrates. As comparatively low performance alternatives to Si NMs, bioresorbable organic semiconductors are also presented, where interest derives from their intrinsic flexibility, low-temperature processability, and ease of chemical modification. Representative examples of encapsulation materials and strategies in passive and active control of device lifetime are then discussed, with various device illustrations. A final section outlines bioresorbable electronics for sensing of various biophysical parameters, monitoring electrophysiological activity, and delivering drugs in a programmed manner.

Fundamental research in chemistry remains essential to the development of this emerging field, where continued advances will increase the range of possibilities in sensing, actuation, and power harvesting. Materials for encapsulation layers that can delay water-diffusion and dissolution of active electronics in passively or actively triggered modes are particularly important in addressing areas of opportunity in clinical medicine, and in secure systems for envisioned military and industrial uses. The deep scientific content and the broad range of application opportunities suggest that research in transient electronic materials will remain a growing area of interest to the chemistry community.



■ INTRODUCTION

Transient electronics is an emerging class of technology characterized by constituent materials that are fully or partially dissolvable or disintegrable by chemical or physical processes, as

Received: October 31, 2017

Published: April 17, 2018



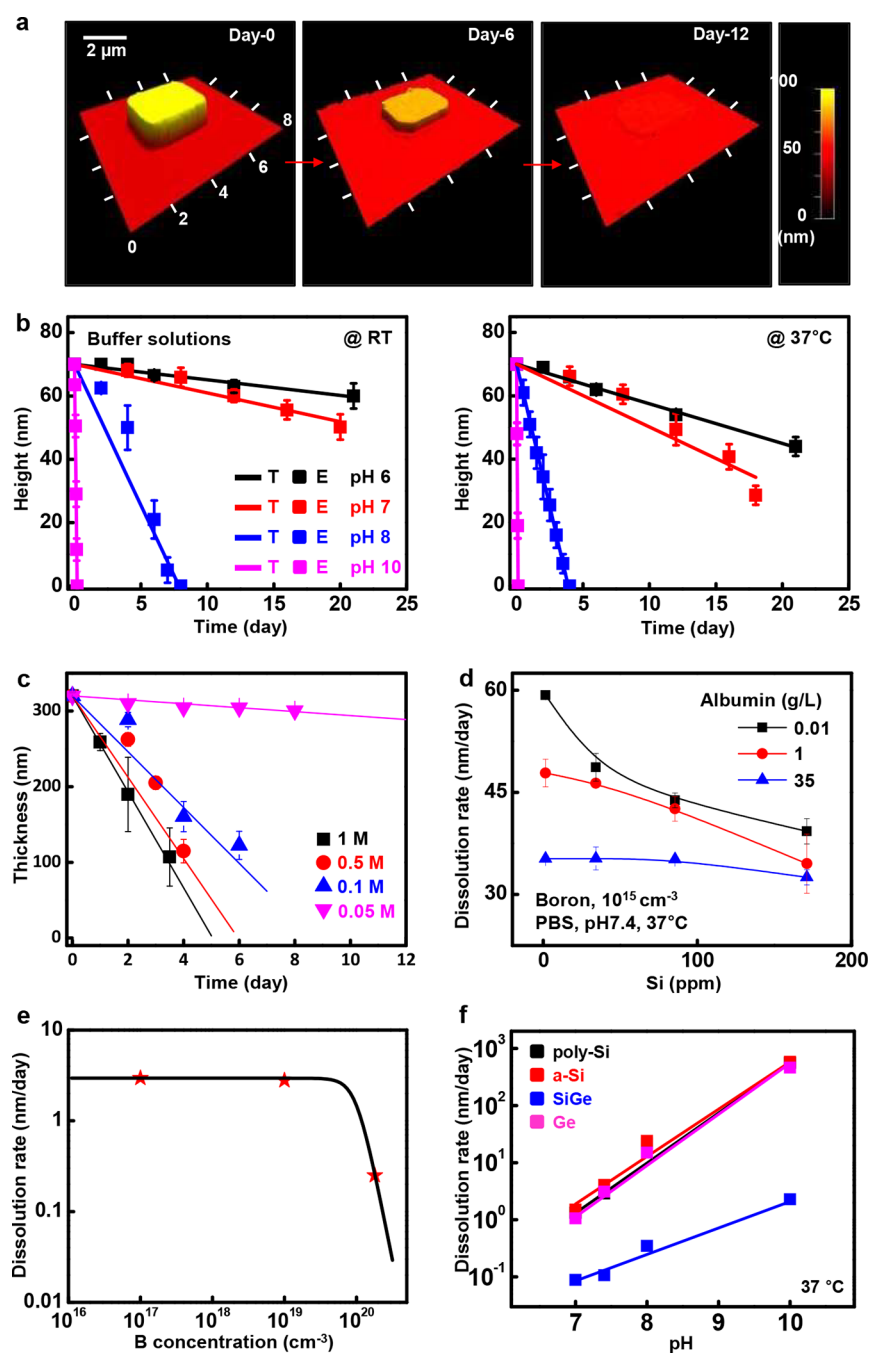


Figure 1. Dissolution chemistry and kinetics of hydrolysis of Si NMs in various aqueous environments. (a) Series of topographical images of a Si NM during hydrolysis in p-PBS. Reproduced with permission from ref 1. Copyright 2012 AAAS. (b) Dissolution kinetics of a Si NM in buffer solutions with various pH at room temperature (left) and body temperature (right, 37 °C) expressed in thickness change. Reproduced with permission from ref 2. Copyright 2014 Wiley. (c) Hydrolysis kinetics of a Si NM in aqueous solution with various concentrations of potassium phosphates at 37 °C. Reproduced with permission from ref 15. Copyright 2015 Wiley. (d) Dependence of the dissolution of Si NMs on the presence of Si(OH)₄ with different protein concentrations. Reproduced with permission from ref 16. Copyright 2017 American Chemical Society. (e) Dopant concentration dependent dissolution of a Si NM in phosphate buffer solution at 37 °C. Reproduced with permission from ref 35. Copyright 2014 American Chemical Society. (f) Dissolution kinetics of poly-Si, a-Si, SiGe, and Ge in buffer solution with different pH at 37 °C. Reproduced with permission from ref 21. Copyright 2015 American Chemical Society.

means to eliminate their existence after a defined period of operation. Application opportunities focus on areas where conventional electronics cannot address key requirements. Examples include environmentally degradable consumer devices that minimize unwanted waste and hardware-oriented secure platforms that physically remove sensitive information or device designs.^{1–3} The most compelling area might be in bioresorbable

electronics, as the basis for active implants that provide diagnostic or therapeutic function during a biological process, such as wound healing, and then disappear entirely to circumvent the need for surgical removal.^{4–6} This natural process of resorption eliminates risk associated with the long-term presence of implantable devices, where infections, immune responses, and steric obstructions represent a few of the many possible types of

complications.⁷ Procedures in surgical extraction have their own risks.⁸ Bioresorbable electronics thereby provide the ultimate solution, where therapeutic function can be analogous to, but distinctly different from, pharmacological approaches to treating disease.

The earliest exploratory efforts in bioresorbable electronics, which included successful demonstrations in animal models, used nonresorbable but thin and ultraminiaturized inorganic electronic components supported by and embedded in bioresorbable polymer materials.⁹ Subsequent research examined the possibility of devices built with bioresorbable organic semiconductors, both synthetic and naturally occurring materials, and nonresorbable metals.^{10–12} The realization that device-grade m-Si nanomembranes (NMs) can undergo hydrolysis to yield benign end products in biofluids established a set of opportunities in high performance classes of electronic systems with versatile functionality.

This Account summarizes recent research efforts in this area, with a focus on these materials and associated underlying chemical processes of resorption, but also with several examples of relevance to biomedical device technology. Some concluding remarks address areas for future work.

CHEMISTRY OF DISSOLUTION OF SILICON NANOMATERIALS

Monocrystalline, electronic-grade silicon is considered to be chemically stable in ambient aqueous environments, due partly to the spontaneous formation of a native oxide on its surface. This notion of stability depends, however, on structural dimensions and observational time scales. Specifically, loss of material from the surface of a bulk silicon wafer (~1 mm thick) immersed in water at rates of a few nanometers per day can be neglected over laboratory time scales; such rates of loss for silicon nanowires, nanoribbons, or nanomembranes will lead to their complete disappearance during similar time frames.¹ In the context of systems described in this Account, active silicon nanostructures dissolve in relevant aqueous environments within several days or weeks, depending on the geometry, the chemical termination of the silicon surface, the type and level of doping of the silicon, and the composition and temperature of the surrounding solutions.

Previous studies of nanoporous silicon (np-Si) and silicon surfaces suggest that the most important reaction is hydrolysis in water to generate orthosilicic acid ($\text{Si}(\text{OH})_4$) and hydrogen as byproducts ($\text{Si} + 4\text{H}_2\text{O} \rightarrow \text{Si}(\text{OH})_4 + 2\text{H}_2$). $\text{Si}(\text{OH})_4$ is a primary form of compounds with general chemical formulas $[\text{SiO}_x(\text{OH})_{4-2x}]_n$,¹³ it is ubiquitously present in natural and biological fluids, commonly at concentrations between 10^0 to 10^1 ppm. Dissolution of silicon nanomaterials, typically several micrograms in total mass for applications discussed here, results in minute changes to this naturally occurring background level. The resultant chemistry for Si NMs (and related ribbon or wire formats) establishes the foundations for high performance classes of electronics that are completely degradable in biological and natural environments. Specifically, the combined use of Si NMs with water-soluble dielectric and conductive materials offer many opportunities.

Figure 1a shows the thickness of a Si NM ($3 \mu\text{m} \times 3 \mu\text{m} \times 70 \text{ nm}$, p-type, $10\text{--}20 \Omega\text{-cm}$) measured at different times of immersion in phosphate buffered saline with pH 7.4 at 37°C (referred to henceforth as p-PBS, for PBS at physiological temperature and pH). The dissolution rate is ~5 nm/day, which results in complete disappearance of this Si NM within 12–13

days.¹ Figure 1b summarizes the dependence of the reaction rate on pH from 6 to 14. Results from the high pH part of this range connect to the well-established kinetics of etching and micromachining of bulk silicon in alkaline solutions. The linear dependence of the thickness (h) on reaction time indicates that the chemistry involves surface erosion, without significant contribution from reactive diffusion of water into the silicon. The simple expression $h = h_0 - Rt$, where h_0 and R are the initial thickness and the reaction rate, respectively, captures the behaviors. Comparison of the rates suggests a scaling relationship with pH in aqueous buffer solutions in a near neutral regime. The functional form is similar to that previously reported for etching of bulk silicon in highly alkaline solutions, $R = k_0[\text{H}_2\text{O}]^4[\text{OH}^-]^{0.25} e^{-E_a/(k_b T)}$, but with a power law exponent for $[\text{OH}^-]$ that is closer to 0.5 than 0.25, possibly due to a surface saturation effect of OH^- in strong alkaline conditions. Here, E_a , k_b , and k_0 are the activation energy and the Boltzmann and reaction constants, respectively. Generally, the rate increases with $[\text{H}_2\text{O}]$ and $[\text{OH}^-]$ due to an increased probability of nucleophilic attack of water and OH^- on the hydrogen terminated Si atoms on the surface. Since the silicon surface during dissolution is terminated with hydrogen,¹⁴ the first step in the production of $\text{Si}(\text{OH})_4$ and H_2 must involve dissociation of the Si–H to form Si–OH.

The chemical complexity increases considerably upon introduction of ions into the surrounding aqueous solutions. As summarized in Figure 1c, certain ions significantly accelerate the rates of reaction,¹⁵ including those (e.g., Na^+ , Ca^{2+} , and Mg^{2+} cations and Cl^- , HCO_3^- , HPO_4^{2-} anions) that are common in environmental and biological fluids at concentrations from 0.1 to >50 g/L. The data show that Si NMs dissolve at ~1 nm/day in low ionic concentrations (e.g., 0.05 M $\text{K}_2\text{HPO}_4/\text{KH}_2\text{PO}_4$) and up to 65 nm/day at high concentrations (e.g., 1 M $\text{K}_2\text{HPO}_4/\text{KH}_2\text{PO}_4$). These variations arise from catalyzing effects of the ions, as suggested by density functional theory (DFT) for the case of anions (HPO_4^{2-} or Cl^-) where interactions with surface Si atoms can weaken nearby Si–Si backbonds.¹⁵ Other simulated biological solutions show different results. For example, remarkably high rates of dissolution (20 to 100 nm/day) occur in bovine serum,^{15,16} modulated by divalent cations (~1 mM Mg^{2+} , Ca^{2+}) and various proteins (~50 g/L in total).¹⁶ Separate experiments designed to reveal the various effects show that CaCl_2 (1 mM) and albumin (35 g/L) in p-PBS increase by ~50% and decrease by ~30% the rate of dissolution, respectively.¹⁶ The latter effect likely arises from adsorption of protein on the silicon surface (0.5 to 1.5 nm, depending on type of protein).¹⁷ The role of silicic acid ($\text{Si}(\text{OH})_4$) as a product of dissolution and a ubiquitous component of natural and biological fluids is also important in this context, as summarized in Figure 1d with three different albumin concentrations in p-PBS.¹⁶ The results show an increased dependence of the dissolution rate on $[\text{Si}(\text{OH})_4]$ with reduced protein concentration, that is, for 0.01 g/L albumin, 59 ± 0.5 to 39 ± 1.9 nm/day and for 35 g/L albumin, 39 ± 0.4 to 33 ± 1.1 nm/day. The dependence on $[\text{Si}(\text{OH})_4]$ can be attributed to reduced step propagation rates and increased activation energy for the formation of vacancy (or highly reactive) sites where dissolution starts to spread.¹⁸

Dopants in the silicon also affect the reaction chemistry. Figure 1e summarizes the rates of dissolution of Si NMs with boron (p-type) dopants at concentrations from 10^{17} to 10^{20} cm^{-3} in phosphate buffer solution (0.1 M, pH 7.4). The rates remain unchanged for concentrations up to 10^{19} cm^{-3} and decrease significantly at 10^{20} cm^{-3} and above. Similar behavior results

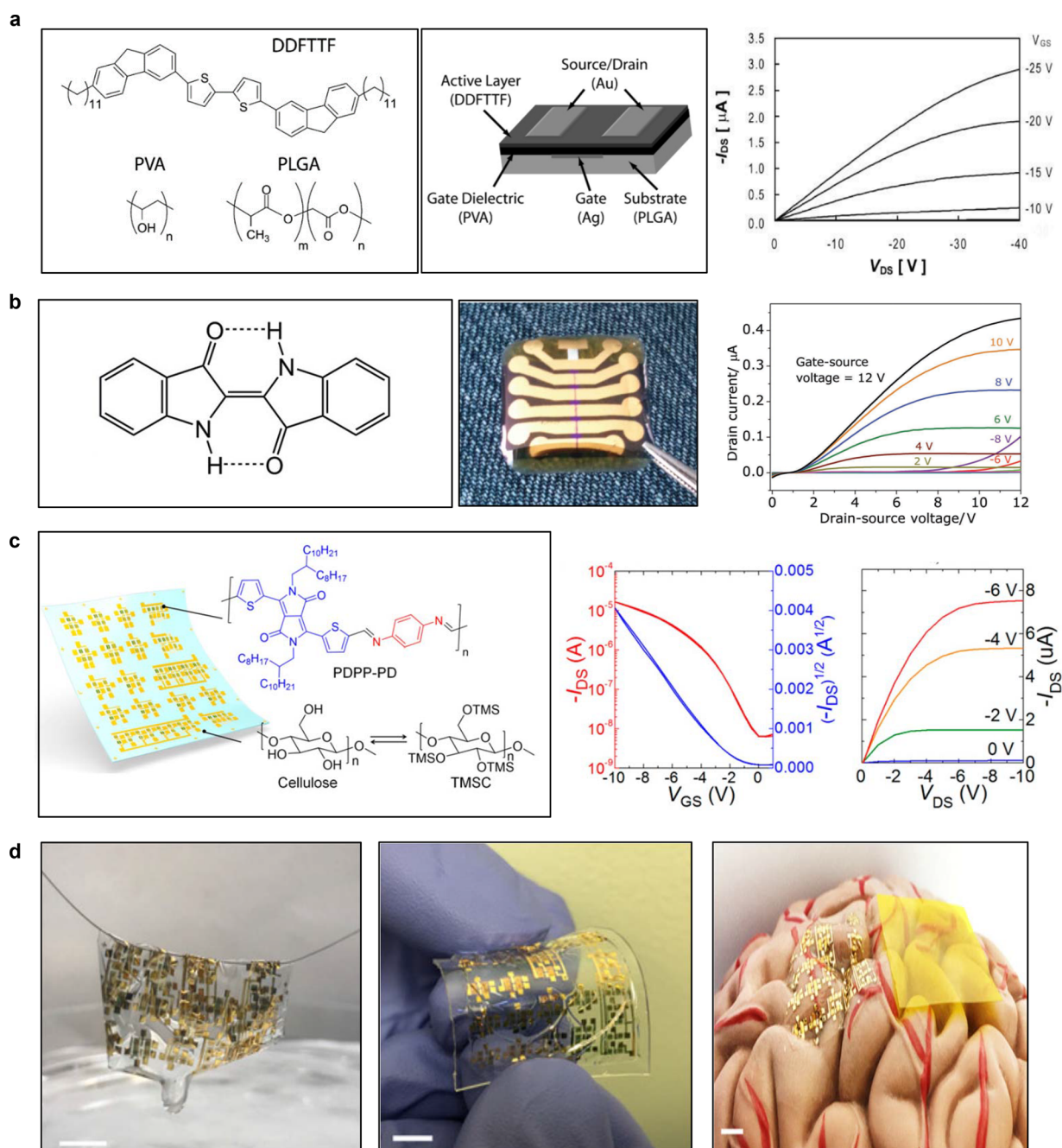


Figure 2. Bioresorbable organic semiconductor and transistor. (a) Bioresorbable organic transistor and its I - V characteristics. Reproduced with permission from ref 10. Copyright 2010 Wiley. (b) Indigo based bioresorbable thin film organic transistor. Reproduced with permission with ref 11. Copyright 2012 Wiley. (c) Illustration of transistor and logic circuit with biodegradable polymer (PDPP-PD) semiconductor on biodegradable cellulose substrates and its electrical performance and (d) series of graphical images describing dissolubility, flexibility, and conformability of the device in panel c. Panels c and d reproduced with permission from ref 12. Copyright 2017 National Academy of Sciences.

from doping with phosphorus (n-type). Such effects are well-known in silicon etching, and they serve as etch stop strategies for chemical micromachining in solutions of KOH (10–57%) or ethylenediamine. The underlying chemistry follows mainly from differences in the native oxide layer that spontaneously forms on the silicon surface. Specifically, ellipsometric measurements show stable, dense layers (~ 1 nm) of SiO_2 on highly doped Si (both boron and phosphorus) when immersed in water, possibly due to barrier-less oxidation pathways facilitated by the presence of dopants or lattice strains induced by the different atomic sizes of silicon and dopants.^{19,20} Lightly doped Si, by comparison,

exhibits porous surface layers of SiO_2 that grow in parallel with dissolution of Si.²⁰ The rate of dissolution of SiO_2 is much slower than that of Si, thereby providing a plausible chemical explanation for the variation in rate with doping level. Additional forms silicon can also be dissolvable. Figure 1f summarizes the dissolution kinetics of poly-Si, a-Si, Ge, and SiGe in phosphate buffer solution (pH 7.4, 0.1 M, 37 °C).²¹

OTHER DISSOLVABLE ELECTRONIC MATERIALS

Recent work shows that Mg, Zn, W, and Mo can serve as bioresorbable metals; systematic studies reveal their dissolution

behavior in thin films and foils.²² These metals react according to $\text{Mg} + 2\text{H}_2\text{O} \rightarrow \text{Mg}(\text{OH})_2 + \text{H}_2$, $\text{Zn} + 2\text{H}_2\text{O} \rightarrow \text{Zn}(\text{OH})_2 + \text{H}_2$, $2\text{W} + 2\text{H}_2\text{O} + 3\text{O}_2 \rightarrow 2\text{H}_2\text{WO}_4$, $2\text{Mo} + 2\text{H}_2\text{O} + 3\text{O}_2 \rightarrow 2\text{H}_2\text{MoO}_4$.²² Fe can dissolve to form hydroxides ($\text{Fe}(\text{OH})_2$ and $\text{Fe}(\text{OH})_3$), although certain byproducts such as Fe_2O_3 and Fe_3O_4 have very low solubility and lead to irregular dissolution.²² Metallic alloys such as those based on Mg and Zn (AZ31B) create possibilities for tunable dissolution.²² The dissolution rates of Mg, Zn, W, Mo, and AZ31B in a representative biofluid (Hank's solution) are 7×10^{-2} , 7×10^{-3} , $(1.7-0.3) \times 10^{-3}$, 3×10^{-4} , and $2 \times 10^{-2} \mu\text{m}\cdot\text{h}^{-1}$ at room temperature.²²

Silicon oxides and nitrides represent attractive choices for bioresorbable dielectrics and encapsulants. For example, p- and n-type metal oxide semiconductor field-effect transistors (MOSFETs) constructed with Si NM channels (300 nm thick), SiO_2 gate dielectric (50 nm thick), and Mg electrodes (300 nm thick) show on/off ratios of greater than $\sim 10^5$ and mobilities of ~ 70 and $\sim 400 \text{ cm}^2 \text{ s}^{-1} \text{ V}^{-1}$, respectively.²³ Dissoluble metallic oxides such as MgO can also be useful. p-Type and n-type MOSFETs with Si NM (~ 300 nm thick), MgO gate dielectric (~ 70 nm thick), and Mg electrodes (~ 250 nm) show on/off ratios of $> 10^5$ and mobilities of 70 and $350 \text{ cm}^2 \text{ s}^{-1} \text{ V}^{-1}$, respectively.¹ The dissolution kinetics of these materials can be strongly affected by morphology, density, and stoichiometry.²⁴ Some unusual choices for dielectrics in bioresorbable systems include egg albumen and magnesium difluoride.^{25,26}

Demonstrated substrates for these applications include thin metal foils and films of polymers (silks, polycaprolactone (PCL), poly(lactic acid) (PLA), poly(lactic-co-glycolic acid) (PLGA, a copolymer of PLA and PGA), and poly(1,8-octanediol-co-citrate) (POC)),^{1,27-30} bio-organics (sodium alginate),³¹ and even foodstuffs (rice paper, cheese, charcoal, seaweed).^{28,32} The substrate also can serve as a water barrier. Some of the most important opportunities are in new materials for substrates and encapsulation layers. Examples of encapsulation strategies follow in later sections.

■ BIOCOMPATIBILITY OF SI NANOMEMBRANES AND OF THEIR DISSOLUTION PRODUCTS

The biocompatibility of Si NMs and hydrolysis byproducts is critically important. Studies of np-Si, which dissolves by the same chemistry but at much higher rates than m-Si, yield some insights.^{33,34} The main product, silicic acid, is a nontoxic small molecule that represents the most common form of bioavailable silicon in the human body (serum contains $11-25 \mu\text{g}$ of silicon/dL).³⁴ Silicic acid does not accumulate within the body but is absorbed by the gastrointestinal tract and is excreted via the urinary pathway.³⁵

Separate studies of the biocompatibility of Si NMs support similar conclusions. When present in cell cultures (metastatic breast cancer cell line (MDA-MB-231)), viability remains above 93% throughout the complete dissolution process.³⁵ Animal model (mice) studies that use Si NMs on silk substrates as subdermal implants indicate no change of body weight and no additional generation of primary immune cells from the axillary and branchial draining lymph nodes.³⁵ Related biocompatibility research involves Si NMs with other transient materials, such as Mg, SiO_2 , and PLGA in the form of functional devices and test platforms. In one case, pressure sensors implanted into the intracranial space of rat models for 2, 4, and 8 weeks indicate no overt reactions of brain glial cells and no focal aggregation of glial cells. Astrocytosis (an increase in the number of astrocyte cells) and microglial activity at the cortical surface remain within

normal limits, indicating no overt immune reaction to the device or its byproducts.⁴

■ ALTERNATIVE BIORESORBABLE SEMICONDUCTORS: ORGANIC POLYMERS

Although Si NMs enable excellent performance characteristics, organic semiconductors offer complementary features such as low-temperature synthesis and processing, comparatively soft/flexible mechanical characteristics, versatile options in surface modification for sensing, and chemically tailored rates of dissolution. Naturally occurring materials provide some interesting options. Figure 2a shows bioresorbable organic thin-film transistors (OTFTs) formed with 5,5'-bis(7-dodecyl-9H-fluoren-2-yl)-2,20-bithiophene (DDFTTF), poly(vinyl alcohol) (PVA), and PLGA as semiconductor, dielectric, and substrate, respectively with Au and Ag electrodes. Although the chemistry associated with its degradation is not well-known, the reactions are likely similar to those for the decomposition of melanin. 5,6-Dihydroxyindole melanin degrades to pyrrole-2,3,5-tricarboxylic acid and pyrrole-2,3-dicarboxylic acid.¹⁰ OTFTs built with these materials can exhibit mobilities up to $\sim 0.25 \text{ cm}^2 \text{ s}^{-1} \text{ V}^{-1}$ and on/off current ratios up to 9×10^3 .¹⁰

Figure 2b provides an additional example in the form of ambipolar field effect transistors built using indigo, a thin layer of AlO_x passivated with tetratetracontane, shellac, and Au for semiconductor, dielectric, substrate, and electrode, respectively.¹¹ Indigo, a dye obtained from the plants *Indigofera tinctoria* and *Isatis tinctoria*, has strong inter- and intramolecular hydrogen bonding and intramolecular π interactions that yield semiconducting properties. The layer of tetratetracontane ($\text{C}_{44}\text{H}_{90}$, TTC) has interactions with the indigo that are favorable for interfacial charge transport. The mobilities for electrons and holes are $1 \times 10^{-2} \text{ cm}^2 \text{ s}^{-1} \text{ V}^{-1}$ and 5×10^{-3} to $1 \times 10^{-2} \text{ cm}^2 \text{ s}^{-1} \text{ V}^{-1}$, respectively. The indigo naturally degrades slowly with the passing of time under the effect of light, humidity, and oxidizing agents.^{36,37} Other natural materials include indanthrene yellow G (vat yellow 1), indanthrene brilliant orange RF (vat orange 3), and perylene diimide as semiconductors and nucleobases (adenine and guanine), sugars (glucose, lactose, sucrose) or caffeine as dielectrics.³⁸

Specially synthesized polymers can offer improved properties. Figure 2c shows the chemical structure of the polymer PDPP-PD, as synthesized by a condensation reaction between *p*-phenylenediamine and DPP-CHO, which is formed by two aldehyde groups to diketopyrrolopyrrole (DPP) at -77°C with catalysis (*p*-toluenesulfonic acid (PTSA)).¹² Reaction of succinic ester and 2-thiophenecarbonitrile in *tert*-amyl alcohol, followed by attaching branched alkyl chains yields DPP. The degradation mechanism for PDPP-PD involves two steps. The imine bonds hydrolyze via acid catalysis. Water then decomposes the DPP monomers through hydrolysis of the lactam rings. The mobility of PDPP-PD ($M_r = 39.6 \text{ kDa}$) can reach $0.21 \pm 0.03 \text{ cm}^2 \text{ s}^{-1} \text{ V}^{-1}$, when used with Al_2O_3 as the gate dielectric (on a cellulose film, 800 nm), Au for gate and source-drain electrodes, and cellulose for substrate. Figure 2d shows the potential use of devices formed with such materials in conformal biomedical applications.

■ COMPONENT AND SYSTEM LEVEL DEMONSTRATIONS

The materials described in the previous sections serve as the foundations for broad classes of electronic devices. In addition to

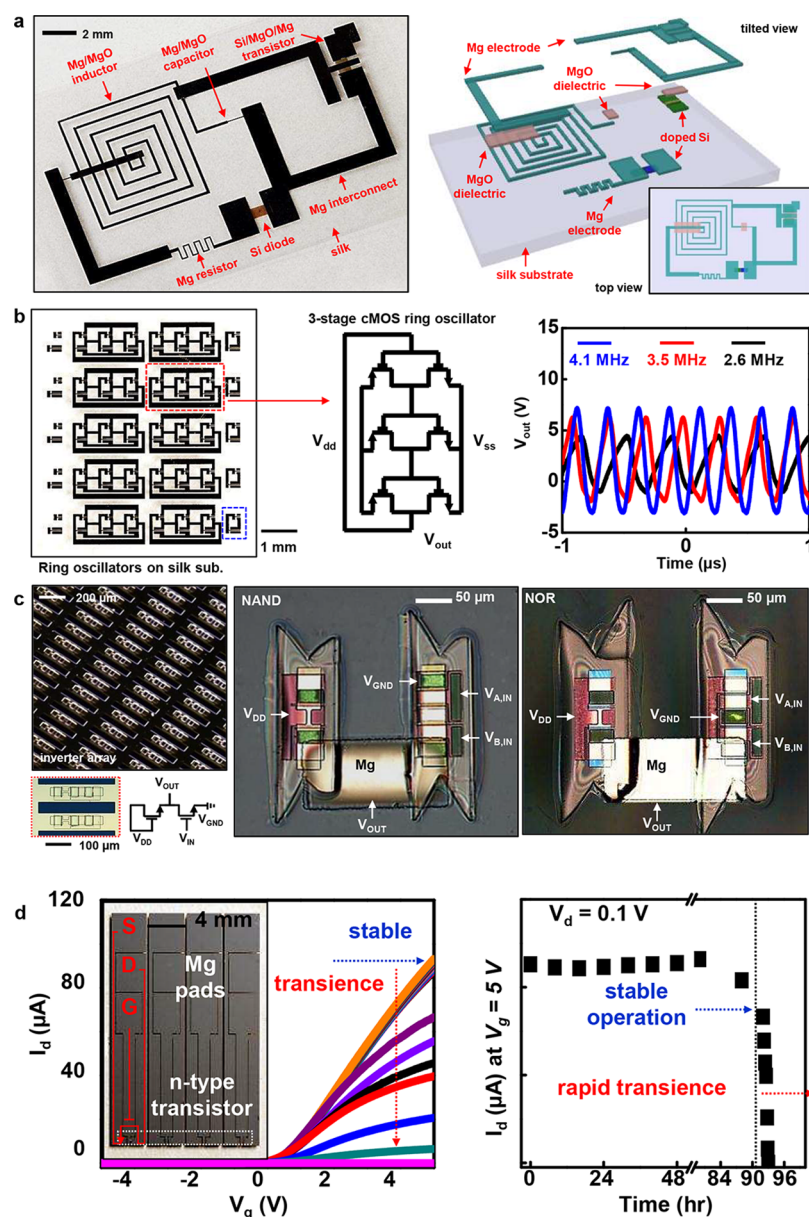


Figure 3. Bioresorbable Si semiconductor electronics from components to systems. (a) A complete set of active (diode, transistor) and passive (inductor, capacitor, resistor) devices using Si NMs, Mg, MgO, and silks demonstrated by a Colpitts oscillator form. Reproduced with permission from ref 1. Copyright 2012 AAAS. (b) Images and properties of transient CMOS inverters (blue dashed square) and ring oscillators (red dashed square). Reproduced with permission from ref 40. Copyright 2013 Wiley. (c) Integrated level of demonstration in logic circuit. Images of an array of inverters (left), NAND (middle), and NOR (right) logic circuit. Reproduced with permission from ref 23. Copyright 2013 Wiley. (d) Two step transient behavior of n-channel transistors encapsulated by MgO and crystalline silk (inset: picture of device) during immersion in DI water. Reproduced with permission from ref 1. Copyright 2012 AAAS.

MOSFETs described previously,^{1,23} electrical double-layer transistors,³⁹ resistive switching memories,³⁰ complementary metal oxide semiconductor (CMOS),²⁸ logic circuits,²³ and others²⁴ are also possible. Figure 3a¹ highlights results from one of the earliest circuit examples, in which a complete set of active (diode, transistor) and passive (inductor, capacitor, resistor) devices based on Si NMs, Mg, MgO, and SiO₂ form a Colpitts oscillator on a thin film of silk fibroin. Each constituent material dissolves in aqueous solutions with characteristic kinetics defined by the chemistry. Figure 3b⁴⁰ shows Si CMOS three-stage ring oscillators formed with similar materials and powered by scavenging circuits, as an additional illustration of the level of complexity that is possible using academic laboratory facilities.

Figure 3c²³ highlights integration of transient transistors into logic circuits such as NAND and NOR gates.

Further scaling in complexity and function is possible by adapting CMOS foundry manufacturing facilities for transient electronics. Recent efforts in this direction establish key capabilities in materials replacement (e.g., tungsten as a bioresorbable metal for interconnects as well as vias), substrate engineering (e.g., silicon on insulator wafers designed to allow release of active devices from the near surface region), and assembly and manipulation (e.g., transfer printing for integration of ultrathin devices onto bioresorbable polymer substrates). Arrays of transient ultrathin silicon components can be formed at a wafer scale using such foundry-based strategies.^{23,41} Undercut

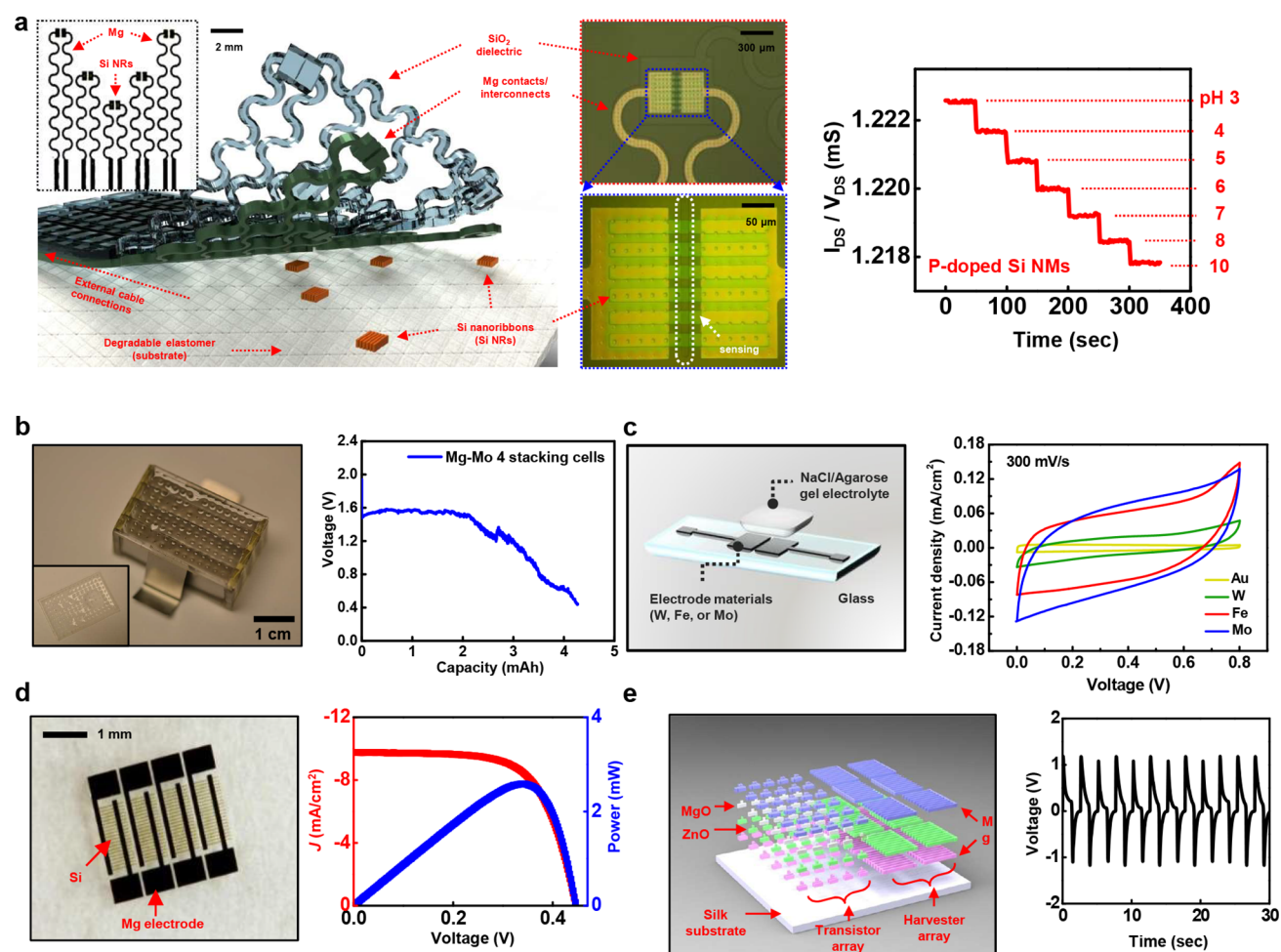


Figure 4. Bioresorbable sensors and energy storage devices. (a) Bioresorbable, stretchable pH sensors using an ion-sensitive field effect transistor (ISFET) with Si nanoribbon, SiO₂ dielectric, and Mg electrode on POC (left). Reproduced with permission from ref 27. Copyright 2015 American Chemical Society. The conductance change of the device at various pH stages (from 3 to 10) (right). (b) Image and discharging behavior of bioresorbable battery pack that consists of four Mg–Mo cells in series with a thin layer of polyanhydride as a spacer. Reproduced with permission from ref 43. Copyright 2014 Wiley. (c) Structure and cyclic voltammetry of bioresorbable planar-type supercapacitor consisting of metal thin-film such as W, Fe, or Mo electrodes and NaCl/agarose gel electrolyte. Reproduced with permission from ref 45. Copyright 2017 Wiley. (d) Image of bioresorbable solar cells that use m-Si NM and Mg electrode (left), and its current density and power as a function of voltage. Reproduced with permission from ref 1. Copyright 2012. AAAS. (e) Bioresorbable thin film transistors and mechanical energy harvesters/strain gauges consist of ZnO (semiconductor/piezoelectric), Mg (conductor), MgO (insulator), and silk (substrate). Output voltage vs time during cycles of bending (right). Reproduced with permission from ref 42. Copyright 2013 Wiley.

etching of the handle wafer of a silicon on insulator (SOI) substrate and manipulation of the released components by transfer printing^{23,41} represent critical steps toward integration with transient substrates.

Encapsulation strategies are critically important to enable reliable operation for a defined time frame. Figure 3d shows an example of the type of two-stage operation that occurs as a result, for the case a N-MOSFET encapsulated with a bilayer of MgO and crystallized silk during immersion in water: stable operation and then rapid degradation after water penetration.¹ This strategy for controlling the functional lifetime relies critically on reproducible materials properties and absence of structural defects such as pinholes²⁴ or variability in molecular chemistry or morphology. The development of new materials for this purpose and of strategies for time-triggered transient systems represent areas of current interest.³

Functional transient materials, together with specialized device designs and fabrication strategies, allow access to many types of sensors,^{1,4,5,27} actuators,^{4,6} and energy-storage devices. Demon-

strated examples of the first device type include thermoresistive temperature gauges and sensors of thermal transport characteristics,⁴ as well as capacitive-type humidity sensors²⁸ that use Si NM electrodes, Mg interconnects, and PLGA substrates; mechanical sensors such as piezoresistive strain gauges,^{1,42} pressure sensors,⁴ accelerometers,⁴ photodiode imagers,¹ and chemical sensors.^{4,27} Figure 4a shows examples of pH sensors that use stretchable ion-sensitive FETs and serpentine interconnecting electrodes on elastic polymer substrates.²⁷

Transient energy sources are essential for many envisioned applications, including remote monitoring devices and biomedical implants. Figure 4b–e summarizes some options, from batteries and supercapacitors to energy harvesters. Galvanostatic pairs of bioresorbable metals such as Mg/Mo (Figure 4b)⁴³ can provide electrochemical sources of electrical power when immersed in electrolyte solution. The performance of single cell batteries that consist of Mg–X (X = Fe, W, or Mo) metal foils with PBS as the electrolyte can yield constant discharge current densities (0.1 mA cm⁻²) and operating voltages of ~0.75, ~0.65,

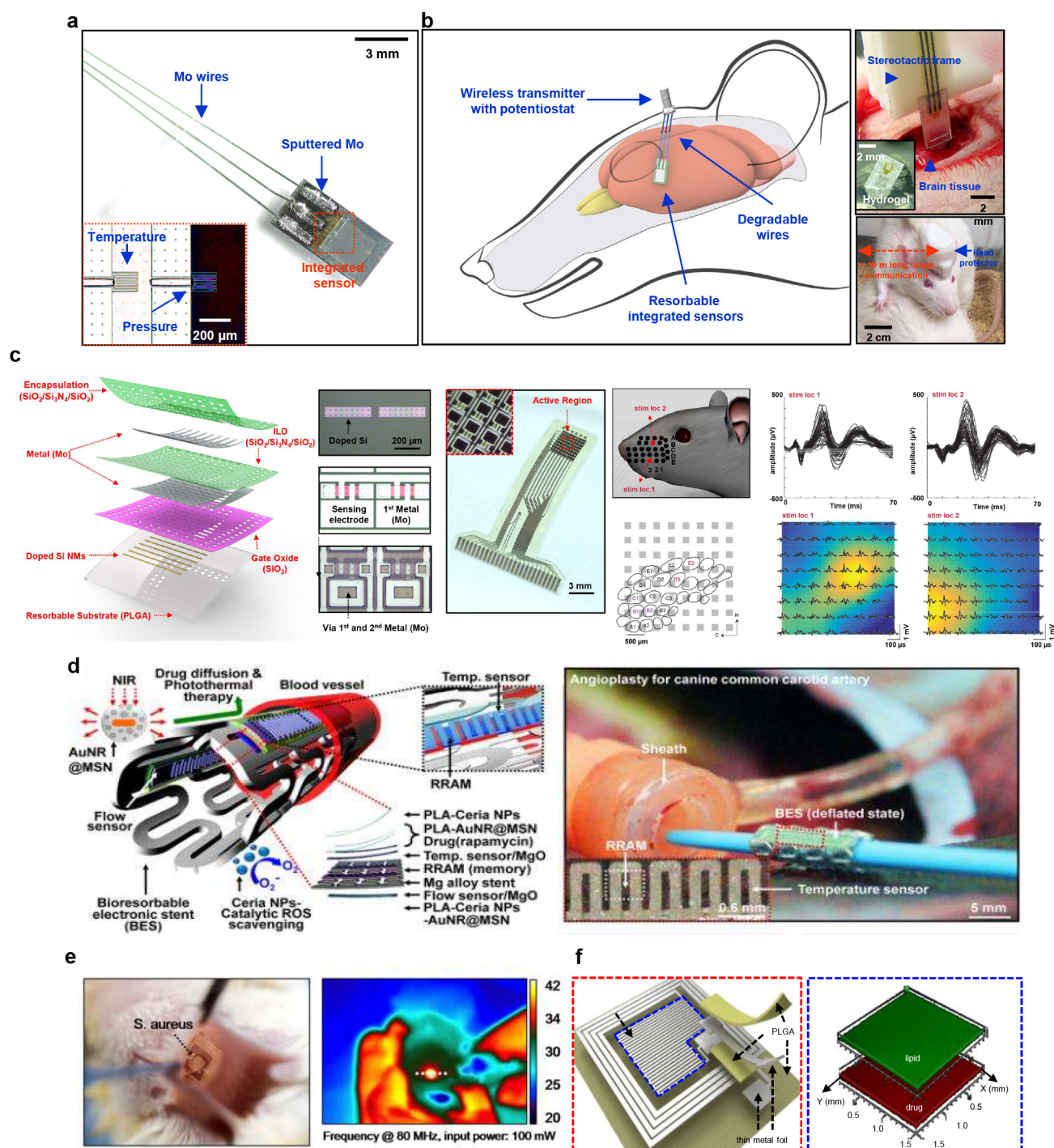
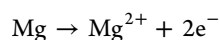


Figure 5. Biomedical applications of bioresorbable devices. (a) Image of bioresorbable pressure and temperature sensors integrated with dissolvable metal (Mo) interconnects. Reproduced with permission from ref 4. Copyright 2016 Nature Publishing Group. (b) Diagram of a bioresorbable temperature and pressure sensor in the intracranial space of a rat model (left). Injectable form of pressure sensor for deep brain monitor (right, upper). Wireless operation of pressure sensor with percutaneous wiring (right, lower). Reproduced with permission from ref 4. Copyright 2016 Nature Publishing Group. (c) Structure and image of a bioresorbable actively multiplexed sensing system. Reproduced with permission from ref 5. Copyright 2016 Nature Publishing Group. (d) Structure and image of bioresorbable electronic stent with multifunctional devices of temperature and flow sensors, memory modules, and therapeutic nanoparticles. Reproduced with permission from ref 47. Copyright 2015 American Chemical Society. (e) Injection ($\sim 5 \mu\text{L}$) of *Staphylococcus aureus* at the device implantation site to mimic surgical-site infections and heat treatments for anti- (left). Reproduced with permission from ref 6. Copyright 2014 National Academy of Sciences. (f) Bioresorbable, wirelessly programmable drug delivery device that exploits thermally activated lipid membranes (right). Reproduced with permission from ref 48. Copyright 2015 Nature Publishing Group. Inductive coil based microheaters formed with Si resistor, Mg electrode, and MgO dielectric on silk (e) and Mo resistor and electrode and PLGA dielectric and substrate (f).

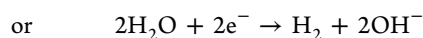
and ~ 0.45 V for Fe, W, and Mo, respectively. Stacking individual Mg–Mo cells in series can increase the output voltage up to 1.6 V

(4 stacking cells) and beyond. The main electrochemical reactions are as follows:

Anode:



Cathode:



(hydrogen evolution)

Other bioresorbable batteries use only organic materials (cellulose membranes, carbon paper electrodes, beeswax impermeable coatings, and organic redox species).⁴⁴ In one case, oxalic acid ($\text{C}_2\text{H}_2\text{O}_4$) and KOH serve as the supporting electrolyte for the positive and negative half-cells, respectively. Prototype devices operate for up to 100 min with an output voltage that can be scaled to match the needs of portable electronic devices (1.5–3.0 V). All materials undergo ~50% biodegradation in anaerobic conditions after 60 days.

Microsupercapacitors (MSCs), as highlighted in Figure 4c, represent complementary technologies for energy storage. Bioresorbable MSCs consist of water-soluble metal (W, Fe, and Mo) electrodes, a biopolymer hydrogel electrolyte (agarose gel), and a PLGA substrate, encapsulated with polyanhydride. The operation exploits the pseudocapacitance of metal-oxide coatings that result from electrochemical corrosion at the interface between the water-soluble metal electrode and the hydrogel (NaCl/agarose) electrolytes. MSCs with Mo interdigitated electrodes and a complete set of degradable components offer areal capacitances of $1.6 \text{ mF}\cdot\text{cm}^{-2}$, energy density of $0.14 \mu\text{W}\cdot\text{h}\cdot\text{cm}^{-2}$, and power density of $1.0 \text{ mW}\cdot\text{cm}^{-2}$.⁴⁵

Transient systems can be designed to capture power from ambient sources. Figure 4d,e shows examples of photovoltaic and piezoelectric systems. Thin layers of m-Si ($\sim 3 \mu\text{m}$ thick) serve as active materials in solar cells where Mg and silk form the electrodes and substrates (Figure 4d).¹ Overall power conversion efficiencies (η) can reach ~3%, limited by incomplete absorption in the thin silicon, with fill factors of 66%. These results are comparable to those of conventional cell designs in this range of thicknesses, when schemes for light-trapping, backside reflection, or antireflection coatings are not used. Harvesting electrical power from mechanical motions is also possible. Dagdeviren et al.⁴² report designs and fabrication schemes for ZnO thin-film mechanical energy harvesters and describe their mechanics and dissolution kinetics. Films of Mg (~ 300 – 400 nm) serve as top and bottom electrodes for a sputter deposited thin film of ZnO (350 – 500 nm) as the piezoelectric component of the device on a silk substrate. In a typical device, voltage and current outputs can reach $\sim 1.14 \text{ V}$ and $\sim 0.55 \text{ nA}$, with a peak output power density of $\sim 10 \text{ nW}/\text{cm}^2$. An alternative harvesting approach⁴⁶ uses triboelectric effects based on contact between the nanostructured surfaces of biodegradable polymers (e.g., PLGA, PVA, PCL, or poly(3-hydroxybutyric acid-co-3-hydroxyvaleric acid) (PHB/V)), where thin films of Mg (50 nm) provide the electrodes. Outputs from such types of generators (size, $2.0 \times 3.0 \text{ cm}^2$) can reach tens of volts.

■ BIORESORBABLE ELECTRONIC IMPLANTS

Implantable devices offer diverse and essential functions for research, advanced diagnosis, and treatment. Traditional permanent electronics provide a range of important functions in this context. In certain cases, this function is most valuable for

finite periods of time, matched to intrinsic biological processes, such as wound healing. Here, removal of the devices after this time period is required to eliminate unnecessary load on the patient and associated risks of uncontrolled migration within the body, pathological tissue responses, and infection. The surgical retrieval procedures, however, can involve complications themselves. Bioresorbable electronics offer a potential solution in this context. The following summarizes recent research demonstrations.

Figure 5a shows a bioresorbable sensor of intracranial pressure, designed for monitoring recovery following a traumatic injury to the brain. The device incorporates a Si NM piezoresistive strain sensor integrated onto a flexible PLGA membrane that forms the top seal of an underlying cavity created on the etched region of the surface of an np-Si substrate or Mg foil.⁴ Figure 5b illustrates its application as an intracranial pressure monitor with an interface to a wireless unit for data transmission. Degradable wires coated with PLGA provide electrical connections between the sensor and external electronics. Studies using a rodent model indicate stable measurement of temperature and pressure in the intracranial space for 3 days.⁴

Active electronic interfaces to the brain also have utility in this context of monitoring during recovery from an injury. Figure 5c shows passively and actively addressed systems for electrophysiological monitoring on the surface of the brain, where the constituent materials and fabrication strategies are similar to those for the devices in Figure 5a.⁵ In these platforms, Si NM electrodes record normal physiologic and epileptiform activity such as electrocorticography (ECoG) and subdermal encephalograms (EEG), in both acute and chronic situations. Heavy doping levels in the Si electrodes lead to relatively slow rates of dissolution in biofluids, thereby enabling use for over 33 days. Systems that include transistors offer active multiplexing for high speed, high resolution mapping. Temporary electronic implants with utility in cardiovascular medicine are also possible such as electronically instrumented bioresorbable stents (Figure 5d).⁴⁷ Such devices use a magnesium alloy mechanical structure with flow and temperature sensors (physiological signal sensing), and an resistive random-access memory (RRAM) array (data storage) based on bioresorbable (Mg, MgO, Zn, ZnO, SiO₂, PLA) materials.

These various systems hint at a future in devices with multimodal operational capabilities and broad utility in biomedicine. In this context, the addition of active, therapeutic function is of interest. One of the earliest examples (Figure 5e) used a wireless power delivery scheme for local heating to eliminate bacterial colonies⁶ that are either inaccessible or nonresponsive to antibiotic treatments. Such systems, constructed with Mg, MgO, and silk, can be left in the body at the end of an intraoperative period. Figure 5f shows an advanced platform of this type, where heating triggers the release of drugs. Wirelessly delivered power induces the expansion of a degradable polymer matrix (e.g., silks, lipids) that contains drugs (e.g., pTH(1–34), dextran, and doxorubicin). In vitro evaluation of a device that delivers doxorubicin, a well-known anticancer chemotherapy drug, to human tumor cells (HeLa) demonstrates the functionality.⁴⁸ Tao et al.⁶ reported the use of silk films doped with ampicillin for thermal release in the context of the timed delivery of antibiotics for respiratory and urinary tract infections, meningitis, salmonellosis, and endocarditis. Bioresorbable forms of on-demand, localized drug delivery systems offer an ideal

scenario for pharmacological treatment of hormone imbalances, malignant cancers, osteoporosis, diabetes, and other diseases.

CONCLUSIONS

Insights from the chemistry of dissolvable semiconductor materials underpin emerging, bioresorbable classes of electronics, with broad potential utility in consumer, military, industrial, and medical systems. The other materials in these platforms are equally important, and they offer many potential avenues for future development in materials chemistry, where high performance operation in sensing, actuation and power harvesting, operation with precisely defined lifetimes, and unusual characteristics such as mechanical flexibility are important end goals. Additional opportunities lie in the development of passively, as well as actively, triggered encapsulation and substrate materials. The rich range of possible research directions, from fundamental studies of the chemistry to innovative engineering of the devices and systems, and the important potential applications in biomedicine suggest a bright future for this field.

AUTHOR INFORMATION

Corresponding Author

*J. A. Rogers. E-mail: jrogers@northwestern.edu.

ORCID

John A. Rogers: 0000-0002-2980-3961

Author Contributions

[†]S.-K.K. and J.K. contributed equally.

Notes

The authors declare no competing financial interest.

Biographies

Seung-Kyun Kang obtained B.S. and Ph.D. degrees in Materials Science and Engineering from the Seoul National University, Korea, in 2006 and 2012. He worked as a postdoctoral researcher at University of Illinois at Urbana–Champaign (2012–2016) and at Northwestern University (2016–2017). He joined Department of Bio and Brain Engineering at KAIST as an Assistant Professor in 2017.

Jahyun Koo received his B.S. and M.S. degrees in Nuclear & Quantum Engineering from KAIST, Korea, in 2010 and 2012. He received his Ph.D. degree in Materials Science and Engineering from KAIST, Korea, in 2016. He is currently a postdoctoral researcher in the Center for Bio-Integrated Electronics at Northwestern University.

Yoon Kyeung Lee received a B.S. in Chemistry Education (2008) and M.S. in Chemistry (2010) from Seoul National University. She is currently a Ph.D. candidate in the Rogers group at University of Illinois at Urbana–Champaign.

John A. Rogers obtained B.A. and B.S. degrees in chemistry and in physics from the University of Texas, Austin, in 1989. He received S.M. degrees in physics and in chemistry (1992) and a Ph.D. in physical chemistry (1995) from MIT. Rogers was a Junior Fellow in the Harvard University Society of Fellows (1995–1997). He joined Bell Laboratories as a Member of Technical Staff in the Condensed Matter Physics Research Department (1997), and served as Director of this department (2000–2002). He spent 13 years on the faculty at the University of Illinois at Urbana–Champaign, most recently as the Swanlund Chair Professor. He currently holds the position of Louis Simpson and Kimberly Querrey Professor at Northwestern University with appointments in the Departments of Materials Science and Engineering and

others, where he also serves as Director of the Center for Bio-Integrated Electronics.

REFERENCES

- (1) Hwang, S.-W.; Tao, H.; Kim, D.-H.; Cheng, H.; Song, J.-K.; et al. A Physically Transient Form of Silicon Electronics. *Science* **2012**, *337*, 1640–1644.
- (2) Hwang, S.-W.; Park, G.; Cheng, H.; Song, J.-K.; Kang, S.-K.; et al. 25th Anniversary Article: Materials for High-Performance Biodegradable Semiconductor Devices. *Adv. Mater.* **2014**, *26*, 1992–2000.
- (3) Hernandez, H. L.; Kang, S.-K.; Lee, O. P.; Hwang, S.-W.; Kaitz, J. A.; et al. Triggered Transience of Metastable Poly(phthalaldehyde) for Transient Electronics. *Adv. Mater.* **2014**, *26*, 7637–7642.
- (4) Kang, S.-K.; Murphy, R. K. J.; Hwang, S.-W.; Lee, S. M.; Harburg, D. V.; et al. Bioresorbable Silicon Electronic Sensors for the Brain. *Nature* **2016**, *530*, 71–76.
- (5) Yu, K. J.; Kuzum, D.; Hwang, S.-W.; Kim, B. H.; Juul, H.; et al. Bioresorbable Silicon Electronics for Transient Spatiotemporal Mapping of Electrical Activity from the Cerebral Cortex. *Nat. Mater.* **2016**, *15*, 782–791.
- (6) Tao, H.; Hwang, S.-W.; Marelli, B.; An, B.; Moreau, J. E.; et al. Silk-based Resorbable Electronic Devices for Remotely Controlled Therapy and In Vivo Infection Abatement. *Proc. Natl. Acad. Sci. U. S. A.* **2014**, *111*, 17385–17389.
- (7) Hall-Stoodley, L.; Costerton, J. W.; Stoodley, P. Bacterial Biofilms: from the Natural Environment to Infectious Diseases. *Nat. Rev. Microbiol.* **2004**, *2*, 95–108.
- (8) Maytin, M.; Epstein, L. M.; Henrikson, C. A. Lead Extraction is Preferred for Lead Revisions and System Upgrades. *Circ.: Arrhythmia Electrophysiol.* **2010**, *3*, 413–424.
- (9) Kim, D.-H.; Viventi, J.; Amsden, J. J.; et al. Dissolvable Films of Silk Fibroin for Ultrathin, Conformal Bio-Integrated Electronics. *Nat. Mater.* **2010**, *9*, 511–517.
- (10) Bettinger, C. J.; Bao, Z. Organic Thin-Film Transistors Fabricated on Resorbable Biomaterial Substrates. *Adv. Mater.* **2010**, *22*, 651–655.
- (11) Irimia-Vladu, M.; Glowacki, E. D.; Troshin, P. A.; Schwabegger, G.; Leonat, L.; et al. Indigo - A Natural Pigment for High Performance Ambipolar Organic Field Effect Transistors and Circuits. *Adv. Mater.* **2012**, *24*, 375–380.
- (12) Lei, T.; Guan, M.; Liu, J.; Lin, H.-C.; Pfattner, R.; et al. Biocompatible and Totally Disintegrable Semiconducting Polymer for Ultrathin and Ultralightweight Transient Electronics. *Proc. Natl. Acad. Sci. U. S. A.* **2017**, *114*, 5107–5112.
- (13) Park, J.-H.; Gu, L.; von Maltzahn, G.; Ruoslahti, E.; Bhatia, S. N.; Sailor, M. J. Biodegradable Luminescent Porous Silicon Nanoparticles for in vivo Applications. *Nat. Mater.* **2009**, *8*, 331–336.
- (14) Watanabe, S.; Nakayama, N.; Ito, T. Homogeneous Hydrogen-Terminated Si(111) Surface Formed Using Aqueous HF Solution and Water. *Appl. Phys. Lett.* **1991**, *59*, 1458–656.
- (15) Yin, L.; Farimani, A. B.; Min, K.; Vishal, N.; Lam, J.; et al. Mechanisms for Hydrolysis of Silicon Nanomembranes as Used in Bioresorbable Electronics. *Adv. Mater.* **2015**, *27*, 1857–1864.
- (16) Lee, Y. K.; Yu, K. J.; Song, E.; Barati Farimani, A.; Vitale, F.; et al. Dissolution of Monocrystalline Silicon Nanomembranes and of Their Use As Encapsulation Layers and Electrical Interfaces in Water-Soluble Forms of Electronics. *ACS Nano* **2017**, *11*, 12562–12572.
- (17) Sofia, S. J.; Premnath, V.; Merrill, E. W. Poly(ethylene oxide) Grafted to Silicon Surfaces: Grafting Density and Protein Adsorption. *Macromolecules* **1998**, *31*, 5059–5070.
- (18) Dove, P. M.; Han, N.; De Yoreo, J. J. Mechanisms of Classical Crystal Growth Theory Explain Quartz and Silicate Dissolution Behavior. *Proc. Natl. Acad. Sci. U. S. A.* **2005**, *102*, 15357–15362.
- (19) Palik, E. D.; Bermudez, V. M.; Glembocki, O. J. Ellipsometric Study of the Etch-Stop Mechanism in Heavily Doped Silicon. *J. Electrochem. Soc.* **1985**, *132*, 135–141.
- (20) Morita, M.; Ohmi, T.; Hasegawa, E.; Kawakami, M.; Ohwada, M. Growth of Native Oxide on a Silicon Surface. *J. Appl. Phys.* **1990**, *68*, 1272–1281.

- (21) Kang, S.-K.; Park, G.; Kim, K.; Hwang, S.-W.; Cheng, H.; et al. Dissolution chemistry and biocompatibility of silicon-and germanium-based semiconductors for transient electronics. *ACS Appl. Mater. Interfaces* **2015**, *7*, 9297–9305.
- (22) Yin, L.; Cheng, H.; Mao, S.; Haasch, R.; Liu, Y.; et al. Dissolvable metals for transient electronics. *Adv. Funct. Mater.* **2014**, *24*, 645–658.
- (23) Hwang, S.-W.; Kim, D.-H.; Tao, H.; Kim, T.-i.; Kim, S.; et al. Materials and Fabrication Processes for Transient and Bioresorbable High-Performance Electronics. *Adv. Funct. Mater.* **2013**, *23*, 4087–4093.
- (24) Kang, S.-K.; Hwang, S.-W.; Cheng, H.; Yu, S.; Kim, B. H.; et al. Dissolution Behaviors and Applications of Silicon Oxides and Nitrides in Transient Electronics. *Adv. Funct. Mater.* **2014**, *24*, 4427–4434.
- (25) He, X.; Zhang, J.; Wang, W.; Xuan, W.; Wang, X.; et al. Transient Resistive Switching Devices Made from Egg Albumen Dielectrics and Dissolvable Electrodes. *ACS Appl. Mater. Interfaces* **2016**, *8*, 10954–10960.
- (26) Zhang, Z.; Tsang, M.; Chen, I. W. Biodegradable Resistive Switching Memory based on Magnesium Difluoride. *Nanoscale* **2016**, *8*, 15048–15055.
- (27) Hwang, S.-W.; Lee, C. H.; Cheng, H.; Jeong, J.-W.; Kang, S.-K.; et al. Biodegradable Elastomers and Silicon Nanomembranes/Nanoribbons for Stretchable, Transient Electronics, and Biosensors. *Nano Lett.* **2015**, *15*, 2801–2808.
- (28) Hwang, S.-W.; Song, J.-K.; Huang, X.; Cheng, H.; Kang, S.-K.; et al. High-Performance Biodegradable/Transient Electronics on Biodegradable Polymers. *Adv. Mater.* **2014**, *26*, 3905–3911.
- (29) Tsang, M.; Armutlulu, A.; Martinez, A. W.; Allen, S. A. B.; Allen, M. G. Biodegradable Magnesium/Iron Batteries with Polycaprolactone Encapsulation: A Microfabricated Power Source for Transient Implantable Devices. *Microsyst. Nanoeng.* **2015**, *1*, 15024.
- (30) Hosseini, N. R.; Lee, J.-S. Biocompatible and Flexible Chitosan-Based Resistive Switching Memory with Magnesium Electrodes. *Adv. Funct. Mater.* **2015**, *25*, 5586–5592.
- (31) Fu, K.; Liu, Z.; Yao, Y.; Wang, Z.; Zhao, B.; et al. Transient Rechargeable Batteries Triggered by Cascade Reactions. *Nano Lett.* **2015**, *15*, 4664–4671.
- (32) Wang, X.; Xu, W.; Chatterjee, P.; Lv, C.; Popovich, J.; et al. Food-Materials-Based Edible Supercapacitors. *Adv. Mater. Technol.* **2016**, *1*, 1600059.
- (33) Archibald, J. G.; Fenner, H. Silicon in Cow's Milk. *J. Dairy Sci.* **1957**, *40*, 703–706.
- (34) Carlisle, E. M. The Nutritional Essentiality of Silicon. *Nutr. Rev.* **1982**, *40*, 193–198.
- (35) Hwang, S.-W.; Park, G.; Edwards, C.; Corbin, E. A.; Kang, S.-K.; et al. Dissolution Chemistry and Biocompatibility of Single-Crystalline Silicon Nanomembranes and Associated Materials for Transient Electronics. *ACS Nano* **2014**, *8*, 5843–5851.
- (36) Vautier, M.; et al. Photocatalytic Degradation of Dyes in Water: Case Study of Indigo and of Indigo Carmine. *J. Catal.* **2001**, *201*, 46–59.
- (37) Poulin, J. Identification of Indigo and its Degradation Products on a Silk Textile Fragment Using Gas Chromatography-Mass Spectrometry. *J. Catal.* **2007**, *32*, 48–56.
- (38) Irimia-Vladu, M.; Troshin, P. A.; Reisinger, M.; Shmygleva, L.; Kanbur, Y.; et al. Biocompatible and Biodegradable Materials for Organic Field-Effect Transistors. *Adv. Funct. Mater.* **2010**, *20*, 4069–4076.
- (39) Guo, J.; Liu, J.; Yang, B.; Zhan, G.; Kang, X.; et al. Low-Voltage Transient/Biodegradable Transistors Based on Free-Standing Sodium Alginate Membranes. *IEEE Electron Device Lett.* **2015**, *36*, 576–578.
- (40) Hwang, S.-W.; Huang, X.; Seo, J.-H.; Song, J.-K.; Kim, S.; et al. Materials for Bioresorbable Radio Frequency Electronics. *Adv. Mater.* **2013**, *25*, 3526–3531.
- (41) Chang, J.-K.; Fang, H.; Bower, C. A.; Song, E.; Yu, X.; Rogers, J. A. Materials and Processing Approaches for Foundry-Compatible Transient Electronics. *Proc. Natl. Acad. Sci. U. S. A.* **2017**, *114*, E5522–E5529.
- (42) Dagdeviren, C.; Hwang, S.-W.; Su, Y.; Kim, S.; Cheng, H.; et al. Transient, Biocompatible Electronics and Energy Harvesters Based on ZnO. *Small* **2013**, *9*, 3398–3404.
- (43) Yin, L.; Huang, X.; Xu, H.; Zhang, Y.; Lam, J.; et al. Materials, Designs, and Operational Characteristics for Fully Biodegradable Primary Batteries. *Adv. Mater.* **2014**, *26*, 3879–3884.
- (44) Esquivel, J. P.; Alday, P.; Ibrahim, O. A.; Fernández, B.; Kjeang, E.; Sabaté, N. A Metal-Free and Biologically Degradable Battery for Portable Single-Use Applications. *Adv. Energy Mater.* **2017**, *7*, 1700275.
- (45) Lee, G.; Kang, S.-K.; Won, S. M.; Gutruf, P.; Jeong, Y. R.; et al. Fully Biodegradable Microsupercapacitor for Power Storage in Transient Electronics. *Adv. Energy Mater.* **2017**, *7*, 1700157.
- (46) Zheng, Q.; Zou, Y.; Zhang, Y.; Liu, Z.; Shi, B.; et al. Biodegradable Triboelectric Nanogenerator as a Life-Time Designed Implantable Power Source. *Sci. Adv.* **2016**, *2*, e1501478.
- (47) Son, D.; Lee, J.; Lee, D. J.; Ghaffari, R.; Yun, S.; et al. Bioresorbable Electronic Stent Integrated with Therapeutic Nanoparticles for Endovascular Diseases. *ACS Nano* **2015**, *9*, 5937–5946.
- (48) Lee, C. H.; Kim, H.; Harburg, D. V.; Park, G.; Ma, Y.; et al. Biological Lipid Membranes for On-Demand, Wireless Drug Delivery from Thin, Bioresorbable Electronic Implants. *NPG Asia Mater.* **2015**, *7*, e227.